Measurement of regional rates of cerebral protein synthesis with L-[1-¹¹C]leucine and PET with correction for recycling of tissue amino acids: I. Kinetic modeling approach

Kathleen C Schmidt, Michelle P Cook, Mei Qin, Julia Kang, Thomas V Burlin and Carolyn Beebe Smith

Unit on Neuroadaptation and Protein Metabolism, Laboratory of Cerebral Metabolism, National Institute of Mental Health, National Institutes of Health, Bethesda, Maryland, USA

Measurements of regional rates of cerebral protein synthesis (rCPS) require correction for the effect of recycling of tissue amino acids back into the precursor pool for protein synthesis. The fraction of the precursor pool derived from arterial plasma, λ, can be evaluated as the steady-state ratio of the specific activity of leucine in the tissue tRNA-bound fraction to that in arterial plasma. While λ can be directly measured in terminal experiments in animals, an alternative method is required for use with PET. We report a method to estimate λ based on a kinetic model of labeled and unlabeled leucine and labeled CO_2 in the tissue. The kinetic model is also used to estimate the amount of labeled protein and rCPS. We measured time courses of [¹⁴C]leucine, [¹⁴C]protein, and ¹⁴CO$_2$ in the blood and brain of anesthetized rats and estimated parameters of the kinetic model from these data. Simulation studies based on the kinetic parameters were then performed to examine the feasibility of this approach for use with L-[1-¹¹C]leucine and PET. λ and rCPS were estimated with low bias, which suggests that PET can be used for quantitative measurement of rCPS with L-[1-¹¹C]leucine and a kinetic modeling approach for correction for recycling of tissue amino acids.

Introduction

Recycling of amino acids derived from protein breakdown in the tissue back into the precursor pool for protein synthesis complicates *in vivo* measurement of rates of incorporation of an amino acid into protein with a radiolabeled tracer amino acid. If plasma is the only source of the amino acid in the tissue, the integrated specific activity of the precursor amino acid in the tissue can be estimated from the measured time course of the amino acid in arterial plasma and a compartmental model of the behavior of the amino acid in the tissue. We have

Correspondence: KC Schmidt, Unit on Neuroadaptation and Protein Metabolism, Laboratory of Cerebral Metabolism, National Institute of Mental Health, Bldg 36, Rm 1A07, 36 Convent Drive, Bethesda, MD 20892-4030, USA.
E-mail: SchmidtK@intra.nimh.nih.gov

shown that, in brain, protein degradation in the tissue is also a significant source of amino acid (Smith *et al*, 1988; Smith and Kang, 2000). Even 60 mins after a bolus injection of a radiolabeled amino acid, the sizeable pool of tissue protein is largely unlabeled and amino acids derived from the steady-state breakdown of unlabeled protein are constantly diluting the specific activity of the precursor amino acid coming from plasma. We accounted for the effect of recycling in the autoradiographic L-[1-¹⁴C]leucine method for measurement of regional rates of cerebral protein synthesis (rCPS) by including in the operational equation a factor, λ, which is the fraction of the precursor pool for protein synthesis derived from arterial plasma; the remainder $(1-\lambda)$ comes from recycling (Smith *et al*, 1988). In application of the autoradiographic method, λ must be evaluated in a separate series of animals by measurement of the ratio of the specific activity of leucine from the tissue tRNA-bound fraction to that of the arterial plasma under steady-state conditions for both labeled and unlabeled leucine. Adaptation of the leucine method for use

618

with PET and L-[1-¹¹C]leucine has been hindered by an inability to measure λ in a clinical setting. Additionally, to determine rCPS, one must be able to determine the amount of labeled protein formed during the experimental interval. In the quantitative autoradiographic L-[1-¹⁴C]leucine method, tissue sections are washed in formalin before autoradiography, thereby washing out free [¹⁴C]leucine and ¹⁴CO₂ in the tissue and leaving only [¹⁴C]protein. Adaptation of the method for use with PET requires that [¹¹C]protein be estimated from total activity measured by the PET scanner by correcting for the presence of [¹¹C]leucine and ¹¹CO₂ in the tissue as well as ¹¹C in blood in the brain. In the present study, we investigated the feasibility of using a kinetic modeling approach for determining λ and rCPS from the measured time courses of leucine and L-[1-¹¹C]leucine in arterial plasma, total activity in whole blood, and total activity in brain regions after injection of L-[1-¹¹C]leucine.

Theory

Kinetic Model for Leucine

The [¹⁴C]leucine method for measurement of rates of leucine incorporation into protein is based on a comprehensive kinetic model (Smith *et al*, 1988; Figure 1). The following assumptions apply: (1) The tissue region is homogeneous with respect to concentrations of amino acids, rates of blood flow, and rates of transport, metabolism, and incorporation of amino acids into protein. (2) The concentration of unlabeled leucine in arterial plasma and rates of amino-acid metabolism and protein synthesis are assumed constant during the experimental period. (3) There is no significant loss of label and no recycling of [¹⁴C]leucine from the radioactive protein within an experimental period of 60 mins. This is a reasonable assumption because the average half-life of protein in brain is several days (Lajtha *et al*, 1976). (4) Concentrations of labeled leucine are sufficiently small that tracer theory holds, and there are no isotope effects associated with its use. The model includes intracellular and extracellular spaces, intracellular compartmentation of free leucine, and admixture of unlabeled leucine released by protein breakdown with amino acids entering the tissue from plasma. In adult rat, it has been shown that there is sufficient admixture to dilute the specific activity of leucine entering the precursor pool in brain from plasma by approximately 40% (Smith *et al*, 1988). Methods to determine rates of cerebral amino-acid incorporation into protein *in vivo* with a tracer amino acid depend on estimation of precursor pool-specific activity from measurements in plasma and will underestimate the true rates unless this dilution is taken into account.
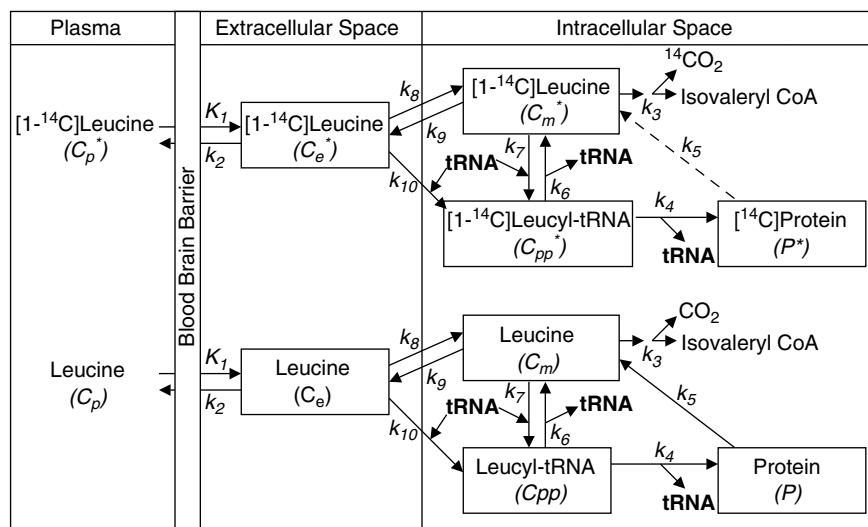

Figure 1 Comprehensive model of leucine in brain. C_p^*, C_e^*, and C_m^* represent concentrations of ¹⁴C-labeled free leucine in plasma, extracellular space, and intracellular space, respectively, and C_p, C_e, and C_m represent their unlabeled counterparts. C_{pp}^* represents the labeled intracellular precursor pool for protein synthesis, that is, [1-¹⁴C]leucyl-tRNA, and P^* represents the pool of labeled leucine in cellular protein. C_{pp} and P are the corresponding unlabeled pools. The constants are: K_1, for carrier-mediated transport of leucine from plasma to tissue; k_2, for transport back from tissue to plasma; k_3, for catabolism of leucine; k_4, for leucine incorporation into protein; k_5, for release of free leucine by protein degradation; k_6, for deacylation of leucyl-tRNA; k_7, for transfer of leucine from the intracellular leucine pool to precursor pool for protein synthesis; k_8, for transport of leucine from extracellular space to intracellular leucine pool; k_9, for transport of leucine from intracellular pool to extracellular space; and k_{10}, for transport of leucine from extracellular space to intracellular precursor pool for protein synthesis. As the average half-life of proteins in brain is several days, it is assumed there is no significant loss of label and no recycling of [¹⁴C]leucine from the radioactive protein within an experimental period of 60 mins, that is, $k_5 P^* = 0$. Although the comprehensive model contains more parameters than can be reliably estimated, it provides a useful description of leucine distribution in the various brain compartments and conversion between compartments. The comprehensive model provided the basis for developing a simplified model for computational purposes.

While the model provides a comprehensive description of leucine kinetics, it contains more unknown parameters than can be reliably estimated. We have, therefore, simplified the model to reduce the number of parameters that need to be estimated, while retaining important features of the original model (Figure 2). The simplified model does not distinguish intra- and extracellular spaces, and the pools of free leucine and tRNA-bound leucine are combined and represented by a single tissue pool. Unlabeled leucine enters the tissue exchangeable pool either from the plasma or through the break-
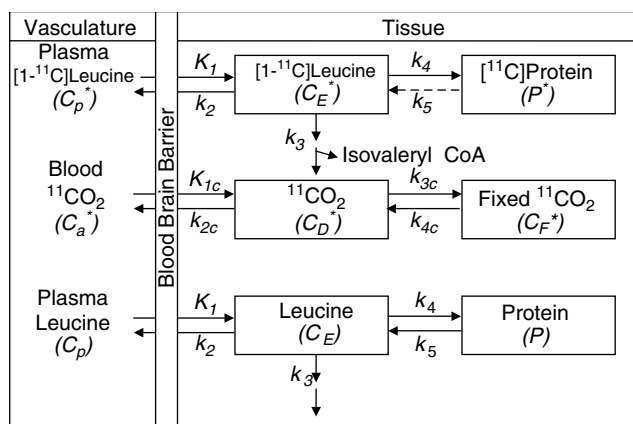

Figure 2 Simplified model of leucine in brain. The simplified model does not distinguish intra- and extracellular spaces, and the pools of free and tRNA-bound leucine are combined into a single tissue pool, represented by C_E^* or C_E, for the labeled or unlabeled exchangeable pools, respectively. C_p^* and C_p represent the arterial plasma concentrations of labeled and unlabeled leucine, respectively. K_1 and k_2 are the rate constants for carrier-mediated transport of leucine from plasma to tissue and from tissue to plasma, respectively. k_3 is the rate constant for the first two steps in the catabolism of leucine, which includes a transamination reaction followed by a rapid decarboxylation. The rate constant for leucine incorporation into protein is represented by k_4, and that for release of free leucine by protein degradation is k_5. P^* and P represent tissue concentrations of labeled and unlabeled proteins, respectively. Unlabeled leucine is assumed to be in a steady state. Due to the long half-life of proteins in brain, it is assumed there is no significant loss of label from the radioactive protein within the experimental period, that is, $k_5P^* = 0$. After an injection of leucine labeled on the carboxyl carbon, the only possible labeled metabolites in brain are α-ketoisocaproic acid (α-KIC), CO_2, and products of CO_2 fixation. Since there is very little labeled α-KIC in brain (Keen et al, 1989), this pool is not explicitly represented in the model and k_3 combines the transamination reaction and decarboxylation, as noted above. Labeled CO_2 can arise either through catabolism of labeled leucine in brain or through influx from the blood after the breakdown of labeled leucine in other tissues; once in the brain, it may be either transported back from brain to blood or fixed in brain. In the model, C_a^* and C_D^* represent the pools of labeled CO_2 in the arterial blood and brain, respectively, and C_F^* represents the concentration of the labeled products of CO_2 fixation in the tissue. K_{1C} and k_{2C} are the rate constants for influx and efflux of labeled CO_2 between brain and blood, respectively, and k_{3C} and k_{4C} represent the rate constants for fixation and loss of fixed CO_2, respectively.

down of protein, and leaves the tissue exchangeable pool by return to the plasma, metabolism, or incorporation into protein. This is described by the first order differential equation

$$\frac{dC_E}{dt} = K_1 C_p(t) - (k_2 + k_3 + k_4)C_E(t) + k_5 P(t) \quad (1)$$

where $C_p(t)$ and $C_E(t)$ are the concentrations of leucine in the arterial plasma and brain exchangeable pool, respectively, and $P(t)$ is the concentration of leucine incorporated into protein. K_1 and k_2 are the rate constants for carrier-mediated transport of leucine from plasma to brain and transport back from brain to plasma, respectively. k_3 is the rate constant for the first two steps in the catabolism of leucine, which include a transamination reaction followed by a rapid decarboxylation. Catabolism appears to be limited by the rate of the transamination reaction in brain (Keen et al, 1989). The rate constants for incorporation of leucine into protein and for the breakdown of protein are k_4 and k_5, respectively. The change in the concentration of protein in the tissue is thus described by

$$\frac{dP}{dt} = k_4 C_E(t) - k_5 P(t) \quad (2)$$

where $C_E(t)$, $P(t)$, k_4 and k_5 are as defined above. Unlabeled leucine, in both the exchangeable pool and in protein, is assumed to be in a steady state, i.e.,

$$\frac{dC_E}{dt} = \frac{dP}{dt} = 0 \quad (3)$$

Labeled leucine has the same kinetics as its unlabeled counterpart, with the exception that it is not in a steady state during the experimental period and there is no significant breakdown of labeled protein, i.e., $k_5 P^*(t) = 0$, where $P^*(t)$ is the concentration of labeled leucine in protein at time t. Therefore, the concentrations of labeled leucine, $C_E^*(t)$, and labeled protein, $P^*(t)$, are given by

$$\frac{dC_E^*}{dt} = K_1 C_p^*(t) - (k_2 + k_3 + k_4)C_E^*(t) \quad (4)$$

$$\frac{dP^*}{dt} = k_4 C_E^*(t) \quad (5)$$

where $C_p^*(t)$ is the concentration of labeled leucine in the arterial plasma.

The only possible labeled metabolites in brain after an injection of leucine labeled on the carboxyl carbon are α-ketoisocaproic acid (α-KIC), CO_2, and products of CO_2 fixation. There is very little labeled α-KIC in brain (Keen et al, 1989), but there remains the possibility of labeled CO_2 and products of CO_2 fixation. Labeled CO_2 can arise either through catabolism of labeled leucine in brain or through influx from the blood after the breakdown of labeled leucine in other tissues. The first step in the catabolic pathway of leucine is a reversible reaction

catalyzed by a branched-chain amino-acid transaminase. The reaction, which takes place primarily in muscle, is the transfer of the α-amino group of leucine to a keto acceptor, usually α-ketoglutarate, to form α-KIC. The α-KIC can be oxidatively decarboxylated to yield CO_2 and isovaleryl CoA, a reaction catalyzed by a branched-chain α-keto acid dehydrogenase enzyme complex primarily in the liver and kidney. Labeled CO_2 produced in this manner can enter the brain via the circulation. Once in the brain, it may return to the blood or be fixed in the brain through anaplerotic reactions associated with tricarboxylic acid intermediates. The equations describing labeled CO_2 kinetics are given by

$$\frac{dC_D^*}{dt} = k_3 C_E^*(t) + K_{1C} C_a^*(t)$$
$$- (k_{2C} + k_{3C})C_D^*(t) + k_{4C}C_F^*(t) \qquad (6)$$

$$\frac{dC_F^*}{dt} = k_{3C}C_D^*(t) - k_{4C}C_F^*(t) \qquad (7)$$

where k_3 and $C_E^*(t)$ are defined above; $C_D^*(t)$ and $C_F^*(t)$ are the brain concentrations of labeled CO_2 and the products of its fixation, respectively; $C_a^*(t)$ is the blood concentration of labeled CO_2; K_{1C} and k_{2C} are the rate constants for influx of labeled CO_2 from blood to brain and efflux of CO_2 from brain to blood, respectively; and k_{3C} *and* k_{4C} are the forward and backward rate constants for fixation of labeled CO_2.

Dilution of the Precursor Pool for Protein Synthesis

In animal studies, the fraction of the precursor pool for protein synthesis that is derived from the arterial plasma, λ, can be evaluated directly as the steady-state ratio of the specific activity of leucine in the tissue tRNA-bound fraction to that in the arterial plasma (Smith *et al*, 1988) as

$$\lambda = \lim_{\substack{t \to \infty \\ C_p^* \text{ and } C_p \text{ constant}}} \left(\frac{C_{pp}^*(t)/C_{pp}(t)}{C_p^*/C_p} \right) \qquad (8)$$

where C_{pp}^* and C_{pp} are the labeled and unlabeled concentrations of t-RNA-bound leucine in the tissue, respectively. Animals are administered a programmed infusion designed to achieve and maintain a constant arterial plasma concentration of labeled leucine and, after a sufficient interval for the brain to reach steady state with the arterial plasma, the specific activities of leucine in plasma and in the brain aminoacyl-tRNA fraction are measured. The equation for λ according to the simplified model (Figure 2) is

$$\lambda = \lim_{\substack{t \to \infty \\ C_p^* \text{ and } C_p \text{ constant}}} \left(\frac{C_E^*(t)/C_E(t)}{C_p^*/C_p} \right) \qquad (9)$$

By solving equations (1) to (5) for the steady-state ratio defined in equation (9), we observe that λ can

also be expressed as the ratio of rate constants

$$\lambda = \frac{k_2 + k_3}{k_2 + k_3 + k_4} \qquad (10)$$

Estimation of Rate Constants and λ

The total activity in the field of view of the PET camera, $C_T^*(t)$, includes tissue activities of labeled leucine, protein, CO_2, and CO_2 fixation products as well as activity in the blood in the brain, i.e.,

$$C_T^*(t) = (1 - V_b)[C_E^*(t) + P^*(t) + C_D^*(t) + C_F^*(t)]$$
$$+ V_b C_b^*(t) \qquad (11)$$

where V_b is fraction of the volume occupied by blood, $C_b^*(t)$ is the total activity in blood, and the remaining terms are as defined previously. In order to use the simplified model equations (4) and (5) to estimate the leucine rate constants K_1, $k_2 + k_3$, and k_4, measured total activity must be precorrected for activity in the blood as well as for labeled CO_2 and its fixation products. For the purpose of rate constant estimation, we assume that labeled CO_2 fixation products are negligible during the experimental interval and that the labeled CO_2 in the brain is rapidly equilibrated with that in the blood, i.e.,

$$C_F^*(t) \approx 0 \text{ and } C_D^*(t) \approx V_D C_a^*(t) \qquad (12)$$

where V_D is the equilibrium distribution ratio for labeled CO_2 given by

$$V_D = \frac{K_{1C}}{k_{2C}} \qquad (13)$$

Equations (4), (5), (11), and (12) form the basis for estimation of the leucine rate constants as detailed in the appendices. λ is then computed from the combination of rate constants shown in equation (10).

Determination of Regional Rates of Cerebral Protein Synthesis

Determination of rCPS with the autoradiographic [¹⁴C]leucine method is based on the principles for assay of rates of chemical reactions with isotopes adapted for the special conditions encountered *in vivo*. The total amount of labeled product specific to the reaction of interest (in this case labeled protein) formed in the selected tissue over an interval of time is divided by the integrated specific activity of the precursor pool over the same interval, that is,

$$rCPS = \frac{P^*(T)}{\left(\int_0^T (C_E^*(t)/C_E) dt \right)} \qquad (14)$$

The numerator of equation (14) represents the amount of labeled protein, which is the only activity remaining in the tissue after the fixation and washing procedure of the autoradiographic [¹⁴C]

leucine method. With PET, $P^*(T)$ can be estimated from total activity (equations (11) and (12)) as

$$P^*(T) \approx \frac{C_T^*(T) - V_b C_b^*(T)}{(1 - V_b)} - V_D C_a^*(T) - C_E^*(T) \quad (15)$$

$C_E^*(T)$ is determined from the time course of the measured labeled leucine in plasma and the rate constants for leucine by the solution of equation (4), viz.,

$$C_E^*(T) = K_1 \int_0^T C_p^*(t) e^{-(k_2+k_3+k_4)(T-t)} dt \quad (16)$$

The integrated specific activity in the precursor pool, the denominator of equation (14), is estimated from the measured time courses of labeled and unlabeled leucine in arterial plasma, the rate constants for leucine by solution of equations (1), (3), and (4), and λ, that is,

$$\int_0^T \frac{C_E^*(t)}{C_E} dt$$

$$= \lambda \left(\int_0^T \frac{C_p^*(t)}{C_p} dt - \int_0^T \frac{C_p^*(t)}{C_p} e^{-(k_2+k_3+k_4)(T-t)} dt \right) \quad (17)$$

Therefore,
rCPS

$$= \frac{\frac{C_T^*(T)-V_b C_b^*(T)}{(1-V_b)} - V_D C_a^*(T) - K_1 \int_0^T C_p^*(t) e^{-(k_2+k_3+k_4)(T-t)} dt}{\lambda \left(\int_0^T \frac{C_p^*(t)}{C_p} dt - \int_0^T \frac{C_p^*(t)}{C_p} e^{-(k_2+k_3+k_4)(T-t)} dt \right)}$$

$$(18)$$

Equation (18) will be referred to as rCPS computational method 'A' because of its analogy with the operational equation of the autoradiographic [^{14}C]leucine method. Values of the rate constants and λ used in equation (18) are those estimated for the individual subject and region. Equation (18) is relatively insensitive to errors in estimates of the individual rate constants K_1, k_2+k_3, and k_4, but requires an accurate estimate of the factor λ.

Regional rates of cerebral protein synthesis may also be determined directly from the estimated rate constants and measured arterial plasma leucine concentration as

$$rCPS = k_4 C_E = \frac{K_1 k_4}{k_2 + k_3} C_p = \left(\frac{K_1 k_4}{k_2 + k_3 + k_4} \right) \frac{C_p}{\lambda} \quad (19)$$

Equation (19) will be referred to as rCPS computational method 'B'; it is derived by solving equations (1)–(3). We note from the ratio on the right in equation (19) that rCPS computed by method 'B' equals the net uptake rate constant for labeled

leucine (in parentheses) multiplied by the plasma unlabeled leucine concentration and corrected for recycling of unlabeled leucine derived from protein breakdown (λ). Regional rates of cerebral protein synthesis computational methods 'A' and 'B' are mathematically equivalent, but are expected to have different sensitivities to errors in the model and data.

In the present study, animal experiments were conducted to estimate the parameters of the kinetic model for leucine and determine the amounts of labeled CO_2 in blood and tissue. From these data, simulation studies were undertaken to investigate the feasibility of using L‑[1‑^{11}C]leucine with dynamic PET scanning to estimate the rate constants, determine λ, and compute rCPS by equation (18) or (19).

Materials and methods

Animals

All procedures were performed in accordance with the National Institutes of Health Guidelines on the Care and Use of Animals and an animal study protocol approved by the National Institute of Mental Health Animal Care and Use Committee. Normal, male Sprague–Dawley rats (Taconic Farms, Germantown, NY, USA) weighing 416 to 480 g were used. Animals were maintained under controlled conditions of normal humidity, temperature, and standard alternating 12‑h periods of light and darkness. Food and water were provided *ad libitum*. With the animals under light halothane anesthesia, catheters were inserted into a femoral artery and vein. Animals were maintained under light halothane anesthesia throughout all experimental procedures. Rectal temperature was continuously monitored and maintained at 37°C by a heat lamp or heat pad.

Chemicals

L‑[1‑^{14}C]leucine (specific activity, 2.15 GBq/mmol) was obtained from Amersham Biosciences Corp., Piscataway, NJ, USA.

Procedures to Determine Time Courses of [^{14}C]leucine, [^{14}C]protein, and $^{14}CO_2$ in Blood and Brain After Injection of L‑[1‑^{14}C]leucine

The experimental period was initiated by an intravenous pulse of L‑[1‑^{14}C]leucine (1.47 to 1.67 MBq in 0.1 mL of normal saline). Six continuous timed arterial blood samples were collected in the first 30 secs; additional timed arterial blood samples were drawn at 0.75, 1, 2.5, 5, 10, 20, 30, 40, 50, and 60 mins or until the end of the experiment. Blood samples were drawn into syringes and ends were immediately capped. Samples were processed in one of three ways: (1) To determine the total concentration of ^{14}C in whole blood, approximately 0.1 mL of blood was transferred to a pre-weighed liquid scintillation vial containing 1 N NaOH, the vial was

reweighed and counted. (2) To determine the concentration of $^{14}CO_2$ in blood, approximately 0.05 mL of blood was injected through the septum of a preweighed sealed vial containing a polyethylene cup with a filter paper soaked with 1 N NaOH, the vial was reweighed and, after allowing 24 h for the evolution of $^{14}CO_2$, the filter paper was removed and counted. (3) To determine plasma concentrations of [^{14}C]leucine and [^{14}C]protein, blood samples were immediately centrifuged to remove the red cells, 20 μL of plasma from each sample was diluted in distilled water and acidified with a solution of 16% (W/V) sulfosalicylic acid to precipitate protein, and the precipitated protein was separated from the acid-soluble free leucine by centrifugation at 10,000 g for 10 mins. Protein pellets were washed twice with 4% sulfosalicylic acid, dissolved in 1 N NaOH, and the concentration of ^{14}C in the dissolved protein fraction was determined by liquid scintillation counting (Packard 2250CA, Packard Instrument Co, Downers Grove, IL). The supernatant fraction and the washes were combined to form the tissue acid-soluble free leucine pools and the concentration of ^{14}C was determined by liquid scintillation counting.

Experiments were terminated at 2.5, 5, 10, 20, 35, or 60 mins by decapitation. The brain was removed rapidly (within 30 secs) and frozen in liquid nitrogen (LN_2). After the brain was frozen completely, it was broken into small pieces while immersed in LN_2. Pieces were transferred to a cryochamber maintained at $-30°C$, rapidly weighed and processed in one of three ways: (1) To determine total tissue ^{14}C concentration, samples ($\sim$20 mg) were solubilized overnight in 1 N NaOH and counted. (2) To determine the tissue $^{14}CO_2$ concentration, samples (20 to 70 mg) were placed in sealed vials and processed as described above for blood samples. (3) To determine brain concentrations of [^{14}C]leucine and [^{14}C]protein, samples (20 to 70 mg) were homogenized in 4% (W/V) sulfosalicylic acid and the precipitated protein was separated from the acid-soluble free leucine by centrifugation at 10,000 g for 20 mins. Protein pellets and supernatant fractions were processed as described above for blood samples.

Alternative Procedure to Determine Time Course of $^{14}CO_2$ in Brain After Injection of L-[1-^{14}C]leucine

To confirm brain $^{14}CO_2$ concentrations, a second group of animals (417 to 581 g) was administered 1.33 to 1.96 MBq L-[1-^{14}C]leucine by i.v. pulse injection. Animals were killed by decapitation at 10, 20, or 60 mins. The brain was removed rapidly (within 30 secs), frozen in LN_2, and broken into small pieces as described above. Frozen samples were transferred to screw-capped microfuge tubes that had been preweighed and precooled in LN_2. Each tube contained a smaller open plastic tube with a 1 N NaOH-soaked filter paper to trap any $^{14}CO_2$ that may escape during reweighing. Microfuge tubes were resubmerged in LN_2 immediately after reweighing. Tissue samples were transferred to Thunberg tubes partially submerged in LN_2 and containing frozen 8% (W/V) sulfosalicylic acid, and sidearms containing NaOH-soaked

filter papers were replaced. While still submerged in LN_2, Thunberg tubes were evacuated and closed before being brought to room temperature. They were left overnight at room temperature for CO_2 to evolve, filter papers were removed, combined with their respective filter papers from the weighing procedure, and counted.

Estimation of Rate Constants of L-[1-^{14}C]leucine

Rate constants K_1, $k_2 + k_3$, and k_4 were estimated by fitting the kinetic model given in equations (4) and (5) to the measured time courses of [^{14}C]leucine in the plasma and [^{14}C]leucine and [^{14}C]protein in brain. Rate constants were constrained so that $\lambda = 0.64$, the value previously measured in the anesthetized rat (Smith *et al*, 1998). The residual sum of squares of the percentage differences between measured and fitted brain [^{14}C]leucine concentrations plus the residual sum of squares of the percentage differences between measured and fitted brain [^{14}C]protein concentrations was minimized by a modification of the method of Koeppe *et al* (1985). Details are provided in Appendix A.

Simulation Studies

Simulations were performed based on the simplified kinetic model for leucine and CO_2 (Figure 2; equations (1)–(7) and (11)). Rate constants K_1, $k_2 + k_3$, and k_4 for L-[1-^{11}C]leucine were those estimated for L-[1-^{14}C]leucine as described above. The fraction of leucine not incorporated into protein that leaves the tissue through efflux, that is, $k_2/(k_2 + k_3)$, was simulated as 10%, 50%, or 90%. Plasma leucine was assumed to be 188 nmol/mL, the average value previously measured in anesthetized rats (Smith *et al*, 1998). In the simulation studies, it was assumed that there is no diffusion limitation of CO_2 into the brain so that its influx rate constant was equal to cerebral blood flow. A value of 1.36 mL g^{-1} min^{-1} was used to approximate K_{1C}; this value is the mean cerebral blood flow reported in normal rats under light halothane anesthesia (Hansen *et al*, 1993). The equilibrium brain:blood partition coefficient for CO_2, (V_D, equation (13)) was assumed equal to the brain:blood ratio of $^{14}CO_2$ concentrations measured 60 mins after a pulse of L-[1-^{14}C]leucine. The rate constant for fixation of CO_2, k_{3C}, was 0.001 or 0.01 min^{-1}, a range chosen to bracket the value of 0.005 min^{-1} estimated from the data of Siesjö and Thompson (1965), and k_{4C} was assumed to be zero. Input functions (labeled and unlabeled leucine in plasma, labeled CO_2 and total activity in whole blood) were the averages of those measured in the rat, normalized to an injected dose of 1.67 MBq (45 μCi) and a body weight of 450 g. Blood volume was assumed to be 2%. For each set of rate constants, the time course of total activity was calculated for a 60-min interval based on a scanning schedule of 10×30, 2×150, and 10×300 secs. Simulated counts were adjusted for ^{11}C decay (half-life 20.38 mins). Zero-mean noise with variance proportional to total counts in each frame of data was added to the total activity. The resultant noise-added data were then

corrected for ¹¹C decay and the rate constants were estimated from linearizations of the simplified kinetic model for leucine as detailed in Appendix B. λ was computed from equation (10), and rCPS was computed by either equation (18) or (19). The procedure was repeated with 1000 random noise samples, and the medians and standard deviations of the estimates of the rate constants, λ, and rCPS were calculated.

Results

Time Courses of [¹⁴C]leucine, [¹⁴C]protein, and ¹⁴CO₂ in Blood and Brain After Injection of ʟ-[1-¹⁴C]leucine

Time courses of [¹⁴C]leucine, [¹⁴C]protein, ¹⁴CO₂, and total ¹⁴C in blood and brain are shown in Figure 3. The peak of [¹⁴C]leucine activity in the plasma occurred 7 ± 3 secs after injection; activity then decreased through the remainder of the experimental interval. Plasma [¹⁴C]protein was negligible until ~ 15 mins postinjection and then increased gradually. Blood ¹⁴CO₂ was low (< 700 Bq/g) throughout. Measured brain total ¹⁴C and [¹⁴C]leucine activities were maximum 2.5 mins postinjection (Table 1; Figure 3B). Total ¹⁴C was approximately constant between 10 and 60 mins, but variance in the measurements was high, probably because of differences between animals as well as differences in specific tissue regions sampled. [¹⁴C]protein in brain increased throughout the 60-min interval. Maximum brain ¹⁴CO₂ activity (274 Bq/g) occurred 10 mins postinjection (Table 1). Brain ¹⁴CO₂ activities represented $8\% \pm 2\%$, $6\% \pm 2\%$, $10\% \pm 1\%$, $6\% \pm 6\%$, $3\% \pm 1\%$, and $5\% \pm 3\%$ of total brain ¹⁴C 2.5, 5, 10, 20, 35, and 60 mins postinjection. The low brain ¹⁴CO₂ activities were confirmed in the second group of animals (Table 1). The brain:blood concentration ratio of ¹⁴CO₂ 60 mins after injection of ʟ-[1-¹⁴C]leucine was 0.53 ± 0.22 ($n = 3$).

Rate Constants of ʟ-[1-¹⁴C]leucine

Rate constants for the simplified kinetic model for leucine, estimated according to the procedure described in Appendix A and constrained so that $\lambda = 0.64$, were $K_1 = 0.059$ mL g⁻¹ min⁻¹ $k_2 + k_3 = 0.15$ min⁻¹, and $k_4 = 0.084$ min⁻¹. Tissue activities predicted by the model with the estimated rate constants and the average input functions are shown in Figure 3B.

Simulation Studies

For all conditions examined estimates of λ had low bias (-5% to $+5\%$), and coefficients of variation were low (5% to 8% at low noise levels, increasing to 17% to 33% at the highest noise levels). The rate constants $k_2 + k_3$ and k_4 were consistently underestimated, but because their estimates were highly correlated ($\rho \approx 0.8$) λ was more accurately estimated
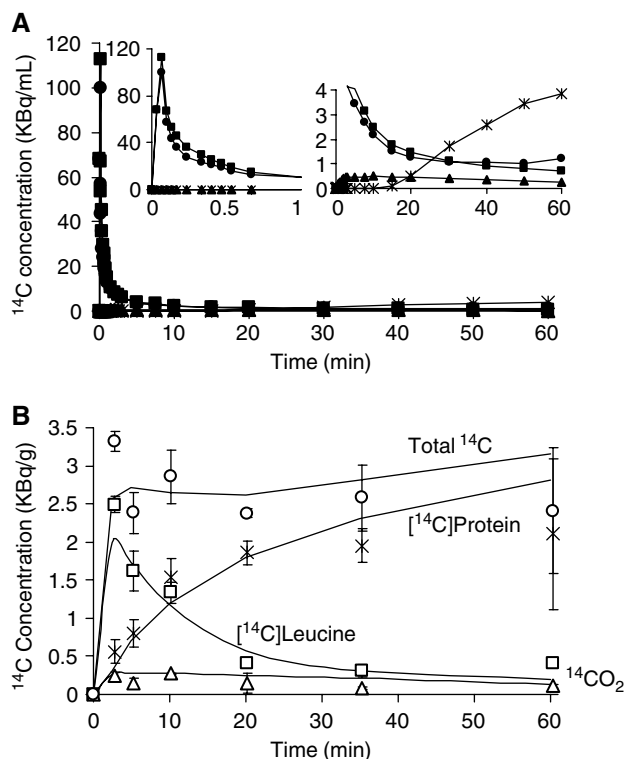

Figure 3 [¹⁴C]leucine, [¹⁴C]protein, and ¹⁴CO₂ in blood and brain after a pulse of ʟ-[1-¹⁴C]leucine. (**A**) Average arterial plasma [¹⁴C]leucine (■) (KBq/mL plasma), arterial plasma [¹⁴C]protein (*) (KBq/mL plasma), arterial blood ¹⁴CO₂ (▲) (KBq/mL blood), and total ¹⁴C activity in arterial blood (●) (KBq/mL blood). Values are means of six to 11 rats ($t \leqslant 20$ mins), four rats (20 mins $< t \leqslant 30$ mins), two rats (30 min $< t \leqslant 60$ mins), where t is the time of the blood sample. As recovery experiments in blood and plasma established that the assay procedure for blood ¹⁴CO₂ converted approximately 1% of label in [¹⁴C]leucine to ¹⁴CO₂, and the assay for plasma protein included approximately 0.1% free [¹⁴C]leucine, the reported data include these corrections. (**B**) Measured brain [¹⁴C]leucine (□), [¹⁴C]protein (*), ¹⁴CO₂ (△), total ¹⁴C activity (○), and model-estimated values (solid lines) based on the simplified kinetic model for leucine (Figure 2). Measured values (KBq/g brain) are the means of two rats at each time point, normalized to an injected dose of 1.67 MBq (45 μCi) ʟ-[1-¹⁴C]leucine and 450 g body weight. Input functions ([¹⁴C]leucine in plasma, ¹⁴CO₂ and total ¹⁴C activity in whole blood) for the model-estimated tissue activities shown were the averages measured in a group of 11 rats shown in (**A**). Rate constants for [¹⁴C]leucine were those estimated from measured time courses of [¹⁴C]leucine and [¹⁴C]protein in brain, that is, $K_1 = 0.059$ mL g⁻¹ min⁻¹, $k_2 + k_3 = 0.15$ min⁻¹, $k_4 = 0.084$ min⁻¹. In this illustration, it is assumed that 50% of the leucine not incorporated into protein that leaves the tissue does so through efflux to the plasma, that is, $k_2 = 0.075$ min⁻¹; the remainder is metabolized, that is, $k_3 = 0.075$ min⁻¹. Different fractions of efflux and metabolism of leucine had only a negligible effect on model-estimated time courses of total activity. The rate constant for influx of ¹⁴CO₂ from blood to brain was assumed to be equal to the weighted average cerebral blood flow in the rat, that is, $K_{1C} = 1.36$ mL g⁻¹ min⁻¹; efflux of ¹⁴CO₂ from brain to blood, k_{2C}, was 2.57 min⁻¹; the volume of distribution of ¹⁴CO₂, V_D, was assumed to be 0.53; k_{3C} was 0.001 min⁻¹ and k_{4C} was assumed to be zero. The concentration of fixed ¹⁴CO₂ and ¹⁴C activity in the blood in the brain are not shown.

than the individual rate constants. As might be expected from the low levels of labeled CO_2 in the tissue, estimates of the rate constants and λ were only negligibly affected by whether the simulated total activity time course was corrected for $^{11}CO_2$ activity before rate constant estimation. Results from one simulation ($K_1 = 0.059\,\text{mL}\,\text{g}^{-1}\,\text{min}^{-1}$, $k_2 = 0.075\,\text{min}^{-1}$, $k_3 = 0.075\,\text{min}^{-1}$, $k_4 = 0.084\,\text{min}^{-1}$, $\lambda = 0.64$; $K_{1C} = 1.36\,\text{mL}\,\text{g}^{-1}\,\text{min}^{-1}$, $K_{2C} = 2.57\,\text{min}^{-1}$, $k_{3C} = 0.001\,\text{min}^{-1}$, $V_D = 0.53$; fitting with no precorrection of simulated total activity for estimated $^{11}CO_2$) are shown in Table 2. Estimates of the rate constants K_1, $k_2 + k_3$ and k_4 decreased with increasing noise level, but estimates of λ increased only slightly. Variances in rCPS increased with increasing noise levels, and those computed with method 'A'

were higher than those determined by method 'B' (Table 2). In all simulations when the $^{11}CO_2$ fixation rate constant was at the lower limit examined ($k_{3C} = 0.001\,\text{min}^{-1}$), bias in rCPS determined by computational method 'A' (equation (18)) ranged from -2% to $+3\%$ at the lowest noise level depending on whether the fraction of leucine not incorporated into protein that leaves the tissue through efflux, i.e., $k_2/(k_2 + k_3)$, was 10%, 50%, or 90%, and whether simulated total activity was precorrected for estimated $^{11}CO_2$. The range increased to -6% to $+6\%$ at higher noise levels. Corresponding biases for rCPS determined by method 'B' were -2% to $+4\%$ at the lowest noise level and -16% to $+3\%$ at the higher noise levels. When the $^{11}CO_2$ fixation rate

Table 1 Total ^{14}C and $^{14}CO_2$ in brain tissue after injection of a bolus of L-[1-^{14}C]leucine[a]

Time (mins)	Total ^{14}C (Bq/g) (Group 1)	$^{14}CO_2$ (Bq/g) (Group 1)[b,d]	$^{14}CO_2$ (Bq/g) (Group 2)[c,d]
2.5	3320 ± 138 (2)	252 ± 49 (2)	
5	2381 ± 265 (2)	146 ± 71 (2)	
10	2860 ± 352 (2)	274 ± 12 (2)	265 ± 26 (4)
20	2377 ± 56 (2)	148 ± 133 (2)	161 ± 3 (2)
35	2582 ± 432 (2)	78 ± 20 (2)	
60	2409 ± 826 (2)	108 ± 31 (2)	122 ± 23 (4)

[a]Values are Means ± SD (number of animals). Data have been normalized to an injected dose of 1.67 MBq (45 μCi) L-[1-^{14}C]leucine and 450 g body weight.
[b]Brain concentrations of $^{14}CO_2$ were measured by placing tissue samples in preweighed sealed vials containing a polyethylene cup with a filter paper soaked with 1 N NaOH, reweighing the vial, and, after allowing 24 h for the evolution of $^{14}CO_2$, removing and counting the filter paper (see Materials and methods).
[c]Brain concentrations of $^{14}CO_2$ were measured by transferring preweighed samples to Thunberg tubes partially submerged in LN_2 and containing frozen sulfosalicylic acid. Sidearms contained NaOH-soaked filter papers. While still submerged in LN_2 Thunberg tubes were evacuated and closed before being brought to room temperature and left overnight for CO_2 to evolve. Filter papers from Thunberg tubes and weighing procedure were combined and counted (see Materials and methods).
[d]There were no statistically significant differences between means of $^{14}CO_2$ measured in the two groups (Student's t-test).

Table 2 Estimated rate constants, λ, and rCPS from simulation study

	K_1 (mL g^{-1} min^{-1})	k_2+k_3 (min^{-1})	k_4 (min^{-1})	λ	rCPS[a] (nmol g^{-1} min^{-1})	rCPS[b] (nmol g^{-1} min^{-1})
			Simulated value			
	0.059	0.150	0.084	0.64	6.2	6.2
Noise level[c]			Model-estimated values[d]			
A	0.061 ± 0.005	0.117 ± 0.030	0.064 ± 0.014	0.65 ± 0.03	6.3 ± 0.8	6.3 ± 0.5
B	0.059 ± 0.007	0.107 ± 0.037	0.061 ± 0.019	0.64 ± 0.05	6.4 ± 1.1	6.3 ± 0.7
C	0.056 ± 0.010	0.087 ± 0.042	0.053 ± 0.024	0.64 ± 0.07	6.5 ± 1.8	6.2 ± 1.1
D	0.050 ± 0.012	0.058 ± 0.046	0.037 ± 0.033	0.66 ± 0.12	6.2 ± 3.1	5.7 ± 2.3

[a]Regional rates of cerebral protein synthesis, computational method 'A' (equation (18)).
[b]Regional rates of cerebral protein synthesis, computational method 'B' (equation (19)).
[c]Zero-mean Gaussian noise with variance proportional to total counts in each frame of data was added to the simulated total activity. Noise levels are in increasing order, with variance at each level doubled over that of the previous level. The coefficients of variation in the first 30-sec frame of data were 17%, 24%, 34%, or 48% for noise levels A, B, C, or D, respectively. The corresponding coefficients of variation in the 55 to 60 mins frame of data were 10%, 14%, 19%, or 27%.
[d]Values are median ± s.d., where 0.7413 × interquartile range is used as a robust estimate of the standard deviation. Parameters used to derive time course of total activity were: for [^{11}C]leucine, $K_1 = 0.059\,\text{mL}\,\text{g}^{-1}\,\text{min}^{-1}$, $k_2 = 0.075\,\text{min}^{-1}$, $k_3 = 0.075\,\text{min}^{-1}$, $k_4 = 0.084\,\text{min}^{-1}$, $\lambda = 0.64$; for leucine, $C_p = 188\,\text{nmol/ml}$; (for $^{11}CO_2$) $K_{1C} = 1.36\,\text{mL}\,\text{g}^{-1}\,\text{min}^{-1}$, $k_{2C} = 2.57\,\text{min}^{-1}$, $k_{3C} = 0.001\,\text{min}^{-1}$, $V_D = 0.53$. While the simulated total activity included $^{11}CO_2$ and products of its fixation, no correction for their presence was made in the fitting procedure, that is, fitting proceeded with $V_D = 0$.

constant was increased to the upper limit examined ($k_{3C} = 0.01\,min^{-1}$) bias in rCPS determined by computational method 'A' ranged from -5% to $+9\%$ at the lowest noise level and -1% to $+12\%$ at higher noise levels; corresponding biases in rCPS computed by method 'B' were $+3\%$ to $+9\%$ and -11% to $+8\%$ at the lowest and higher noise levels, respectively. In almost all simulations, variances in rCPS determined by computational method 'B' were lower than those determined by method 'A'.

Discussion

In the present study, we have introduced a new method for determination of λ, a number that represents the fraction of leucine in the precursor pool for protein synthesis that is derived from arterial plasma. As rates of cerebral protein synthesis determined with L-[1-^{14}C]leucine or L-[1-^{11}C]leucine are inversely proportional to λ, rCPS may be significantly underestimated if this factor is not taken into account. In rats, for example, λ has been determined to be 0.58 in the awake animal (Smith et al, 1988) and 0.64 in the thiopental-anesthetized animal (Smith et al, 1998); failure to take it into account would result in $\sim 40\%$ underestimation of rCPS. Previously, determination of λ was only possible by direct biochemical assay. No method suitable for PET studies had been reported; this presented a major obstacle to the development of a method for measuring rCPS in human studies. The method proposed here is based on a kinetic model for leucine and requires that the time course of brain activity after injection of labeled leucine be measured, which can be readily achieved with PET. The present simulation studies suggest that λ can be reliably estimated, even from noisy PET data.

The kinetic modeling method for determination of λ (equation (10)) is based on the definition of λ in equation (8) and is dependent on three premises. The first is that there is no isotope effect, that is, identical rate constants operate on both labeled and unlabeled leucine. The second is that there is a steady state for unlabeled leucine in the tissue, that is, that there is no net change in the sizes of either the exchangeable pool or the pool of leucine incorporated into protein. Rates of protein synthesis and protein degradation are therefore equal. The third premise is that the steady state for the labeled leucine is an *apparent* steady state because it pertains to the free and tRNA-bound leucine only, not the protein bound (Smith et al, 1998). We have assumed that $k_5 P^* = 0$ because the average half-life of protein in brain is several days (Lajtha et al, 1976), but $k_4 C_E^* \neq 0$. It is this difference in the conditions for the labeled and unlabeled species that forms the basis for the definition of λ as a ratio of rate constants.

The second challenge to adapting the [^{14}C]leucine autoradiographic method to PET was that of determining the amount of labeled protein synthesized during the experimental interval. In the autoradiographic method, tissue sections are fixed and washed before autoradiography, thereby removing both free leucine and labeled metabolites. With PET, however, only total activity in the field of view is measured with the PET camera, and the data must be corrected for labeled free leucine, metabolites, and blood in the tissue. The experimental design of giving a pulse of leucine and estimating the amount of protein synthesized after a 1-h interval serves to allow the free leucine in the tissue to clear so that it is only a small fraction of the total activity at the end of the interval. Errors in estimation of free leucine, therefore, do not have a large impact on determinations of rCPS when computational method 'A' is applied. However, measurement of the full time course of tissue activity, which is not possible with the autoradiographic method, is possible with PET; this allows determination of rCPS directly from the estimated rate constants and the arterial plasma leucine concentration, that is, by use of computational method 'B'. Comparisons of rCPS computational methods 'A' and 'B' should be interpreted with caution, however, as the present simulation examined only errors due to noise in the time–activity curves and due to ignoring the presence of labeled CO_2 and its fixation products; it did not consider the effects of other sources of error. Results on measured PET data will provide more meaningful comparisons.

Our data indicate that tissue levels of $^{14}CO_2$ are low throughout the 60-min interval after injection of L-[1-^{14}C]leucine. Tissue levels of $^{14}CO_2$ reach a peak of 10% of total activity 10 mins postinjection. These levels were somewhat lower and peaked somewhat later than those measured in conscious rats (Keen et al, 1989). The present simulation study based on the low levels of tissue $^{14}CO_2$ measured in rats indicates that the presence of labeled CO_2 can be ignored in estimation of λ and rCPS without introducing significant bias. Higher levels of labeled CO_2 in brain or increased fixation rates, if present, for example, as a result of hypoglycemia, very high blood concentrations of branched-chain amino acids, or elevated tissue ammonia might be at least partially corrected by means of measurements of labeled CO_2 in the blood, although this remains to be tested.

The kinetic model used in the present study differs from the model proposed for use with L-[1-^{11}C]leucine by Hawkins et al (1989). Hawkins et al (1989) did not address recycling of unlabeled leucine derived from protein breakdown into the precursor pool for protein synthesis. Without correction for recycling, computed rates of cerebral protein synthesis are underestimated, and one cannot distinguish true changes in *rCPS* from

apparent changes resulting from alterations in λ. Additionally, the model of Hawkins et al (1989) differs in the description of labeled metabolites in brain. Our model accounts for $^{11}CO_2$ that may enter the brain from blood as well as $^{11}CO_2$ produced by metabolism of [^{11}C]leucine in the brain, whereas the model of Hawkins et al (1989) considers the latter to be the only source of $^{11}CO_2$. We have found that this compartment is sufficiently small that it can be ignored, at least under the conditions of our study. Thus, a two-tissue compartmental model effectively describes total activity. By contrast, the model of Hawkins et al (1989) in studies of monkeys predicted a larger metabolite pool with slower turnover; this may result in lower estimates of the amount of leucine incorporated into protein than those provided by our model. Studies in primates, essential to validate the use of the presently proposed kinetic model, have been performed and are reported elsewhere (Smith et al, 2005).

The present study has known limitations. The simplified kinetic model did not fully describe the time courses of free [^{14}C]leucine and [^{14}C]protein measured in the rat. The high degree of variability in the tissue activities, particularly [^{14}C]protein activity measured at late times, compounds the difficulty of obtaining good fits with the kinetic model. The high variability might be due to the necessity of using a separate group of animals at each time point as well as the difficulty of sampling comparable tissue regions in each animal. In the present study, measured [^{14}C]protein increases more rapidly than estimated [^{14}C]protein in early intervals after injection, but the pattern reverses at later times. This precursor-product pattern is consistent with the presence of tissue heterogeneity and application of a kinetic model based on the assumption of tissue homogeneity, as previously seen in [^{14}C]deoxyglucose studies (Schmidt et al, 1995). Other simplifications of the kinetic model, for example, the combination of the free and tRNA-bound leucine pools into a single precursor pool in brain, might also have affected the goodness-of-fit. The effects of tissue heterogeneity and other model simplifications on estimation of λ and rCPS are yet to be determined. Additionally, the value of λ in the halothane-anesthetized rat may differ from that in the thiopental-anesthetized rat. In the present simulation study, we relied on rate constants for influx and efflux of labeled CO_2 between blood and brain that were consistent with the observed data, but we did not measure brain $^{14}CO_2$ activities at sufficiently early times to enable direct estimation of CO_2 rate constants. Simulations with slower kinetics of labeled CO_2, however, did not yield notably different estimates of λ and rCPS (data not shown), probably because of the low levels of labeled CO_2 in the tissue.

Results of the present study suggest that PET measurement of regional cerebral protein synthesis with L-[1-^{11}C]leucine and a kinetic modeling approach to correct for recycling of tissue amino acids is feasible. Validation studies were, therefore, performed in primates to compare biochemical determinations of λ with estimates from dynamic PET studies and to compare rCPS determined with the L-[1-^{14}C]leucine autoradiographic method with that determined with L-[1-^{11}C]leucine and PET; results are reported in our companion paper (Smith et al, 2005).

Acknowledgements

References

Hansen TD, Warner DS, Traynelis VC, Roach RM, Todd MM (1993) Cerebral blood flow in a rat glioma model during halothane anesthesia. J Neurosurg Anesth 5:187–93

Hawkins RA, Huang S-C, Barrio JR, Keen RE, Feng D, Mazziotta JC, Phelps ME (1989) Estimation of local cerebral protein synthesis rates with L-[1-^{11}C]leucine and PET: methods, model, and results in animals and humans. J Cereb Blood Flow Metab 9:446–60

Keen RE, Barrio JR, Huang S-C, Hawkins RA, Phelps ME (1989) In vivo cerebral protein synthesis rates with leucyl-transfer RNA used as a precursor pool: determination of biochemical parameters to structure tracer kinetic models for positron emission tomography. J Cereb Blood Flow Metab 9:429–45

Koeppe RA, Holden JE, Ip WR (1985) Performance comparison of parameter estimation techniques for the quantitation of local cerebral blood flow by dynamic positron computed tomography. J Cereb Blood Flow Metab 5:224–34

Lajtha A, Latzkovits L, Toth J (1976) Comparison of turnover rates of protein of brain, liver, and kidney in mouse in vivo following long term labeling. Biochim Biophys Acta 425:511–20

Schmidt KC, Smith CB (2003) Kinetic modeling approach to measurement of regional rates of cerebral protein synthesis with L-[1-^{11}C]leucine and PET: estimation of the correction factor for recycling of tissue amino acids. J Cereb Blood Flow Metab 23(Suppl 1):681

Schmidt KC, Mies G, Dienel GA, Cruz NF, Crane AM, Sokoloff L (1995) Analysis of time courses of metabolic precursors and products in heterogeneous rat brain tissue: limitations of kinetic modeling for predictions of intracompartmental concentrations from total tissue activity. J Cereb Blood Flow Metab 15:474–84

Siesjö BK, Thompson W (1965) The uptake of inspired $^{14}CO_2$ into the acid-labile, the acid-soluble, the lipid, the protein and the nucleic acid fractions of rat brain tissue. Acta Physiol Scand 64:182–92

Smith CB, Deibler GE, Eng N, Schmidt K, Sokoloff L (1988) Measurement of local cerebral protein synthesis in vivo: influence of recycling of amino acids derived from protein degradation. Proc Natl Acad Sci USA 85:9341–5

Smith CB, Eintrei C, Kang J, Sun Y (1998) Effects of thiopental anesthesia on local rates of cerebral protein synthesis in rats. Am J Physiol 274:E852–9

Smith CB, Kang J (2000) Cerebral protein synthesis in a genetic mouse model of phenylketonuria. *Proc Natl Acad Sci USA* 97:11014–9

Smith CB, Schmidt KC, Burlin T, Cook M, Kang J, Qin M, Sokoloff L, Saunders R, Bacher J, Carson R, Channing M, Eckelman W, Herscovitch P, Vuong B-K, Laverman P (2005) Measurement of regional rates of cerebral protein synthesis with L-[1-¹¹C]leucine and PET with correction for recycling of tissue amino acids: II. Validation in rhesus monkeys. *J Cereb Blood Flow Metab* (in press)

Appendix A: Estimation of Rate Constants from Biochemical Determinations of Labeled Leucine and Protein

From equations (4) and (5) and zero initial conditions, the model equations for the amount of labeled leucine, C_E^*, and labeled protein, P^*, in the tissue at time T can be written as

$$C_E^*(T) = K_1 \int_0^T C_p^*(t) e^{-(k_2+k_3+k_4)(T-t)} dt \qquad (A1)$$

and

$$P^*(T) = \left(\frac{K_1 k_4}{k_2 + k_3 + k_4} \right)$$
$$\times \left(\int_0^T C_p^*(t) dt - \int_0^T C_p^*(t) e^{-(k_2+k_3+k_4)(T-t)} dt \right)$$

Since $\lambda = (k_2 + k_3)/(k_2 + k_3 + k_4)$, the above equation can be rewritten as

$$P^*(T) = K_1(1 - \lambda)$$
$$\times \left(\int_0^T C_p^*(t) dt - \int_0^T C_p^*(t) e^{-(k_2+k_3+k_4)(T-t)} dt \right)$$
$$(A2)$$

Observe from equations (A1) and (A2) that, if $(k_2 + k_3 + k_4)$ and λ were known, then the above integrals could be computed and $C_E^*(T)$ and $P^*(T)$ would be linear in the parameter K_1. This is the basis of the linear least-squares search method of Koeppe *et al* (1985), which was used in the present study to estimate the parameters K_1, $k_2 + k_3$, and k_4, constrained so that $\lambda = 0.64$, the value previously measured in the anesthetized rat (Smith *et al*, 1998). The vectors of data observations are

$$\boldsymbol{C_E^*} = \begin{bmatrix} C_{E1}^*(T_1) \\ C_{E2}^*(T_2) \\ \cdots \\ C_{En}^*(T_n) \end{bmatrix} \text{ and } \boldsymbol{P^*} = \begin{bmatrix} P_1^*(T_1) \\ P_2^*(T_2) \\ \cdots \\ P_n^*(T_n) \end{bmatrix}$$

where $C_{Ei}^*(T_i)$ and $P_i^*(T_i)$ are the tissue activities of labeled leucine and protein, respectively, measured in animal i at time T_i. For the fixed value of λ and a range of values of $\beta_j = k_{2j} + k_{3j} + k_{4j}$, the vectors

$$\boldsymbol{X_c^{(j)}} = \begin{bmatrix} \int_0^{T_1} C_{p1}^*(t) e^{-\beta j(T1-t)} dt \\ \int_0^{T_2} C_{p2}^*(t) e^{-\beta j(T2-t)} dt \\ \cdots \\ \int_0^{T_n} C_{pn}^*(t) e^{-\beta j(Tn-t)} dt \end{bmatrix}$$

and

$$\boldsymbol{X_P^{(j)}} = \begin{bmatrix} (1 - \lambda)\left(\int_0^{T_1} C_{p1}^*(t) dt - \int_0^{T_1} C_{p1}^*(t) e^{-\beta j(T1-t)} dt \right) \\ (1 - \lambda)\left(\int_0^{T_2} C_{p2}^*(t) dt - \int_0^{T_2} C_{p2}^*(t) e^{-\beta j(T2-t)} dt \right) \\ \cdots \\ (1 - \lambda)\left(\int_0^{T_n} C_{pn}^*(t) dt - \int_0^{T_n} C_{pn}^*(t) e^{-\beta j(Tn-t)} dt \right) \end{bmatrix}$$

were calculated, where $C_{pi}^*(t)$ is the labeled leucine in the arterial plasma of animal i at time t. For each j, a linear least-squares algorithm was used to find the value $K_1^{(j)}$ that minimizes

$$WRSS^{(j)} = \|\mathbf{W}(\boldsymbol{y} - \boldsymbol{X}^{(j)} \boldsymbol{K}_1^{(j)})\|_2^2$$

where $\boldsymbol{y} = \begin{bmatrix} \boldsymbol{C_E^*} \\ \boldsymbol{P^*} \end{bmatrix}$, $\boldsymbol{X}^{(j)} = \begin{bmatrix} \boldsymbol{X_C^{(j)}} \\ \boldsymbol{X_P^{(j)}} \end{bmatrix}$, and $\mathbf{W}$ is the matrix of weights, that is,

$$W_{mn} = \begin{cases} 1/y_m & \text{if } m = n \\ 0 & \text{if } m \neq n \end{cases}$$

Finally, the index j was chosen at which $WRSS^{(j)}$ was minimum. Then $K_1 = K_1^{(j)}$, $k_2 + k_3 = \lambda \beta_j$, and $k_4 = (1 - \lambda)\beta_j$.

Appendix B: Estimation of Rate Constants of [¹¹C]leucine from Dynamic PET Data

The simplified kinetic model for leucine describes the labeled free leucine in the tissue, $C_E^*(t)$, and the labeled protein in the tissue, $P^*(t)$, by the following set of differential equations:

$$\frac{dC_E^*}{dt} = K_1 C_p^*(t) - (k_2 + k_3 + k_4)C_E^*(t) \qquad (B1)$$

$$\frac{dP^*}{dt} = k_4 C_E^*(t) \qquad (B2)$$

Define C_i^* as the sum of the labeled free leucine and protein in the tissue, that is,

$$C_i^*(t) = C_E^*(t) + P^*(t). \qquad (B3)$$

Then, from equations (B1) and (B2)

$$\frac{dC_i^*}{dt} = \frac{dC_E^*}{dt} + \frac{dP^*}{dt} = K_1 C_p^*(t) - (k_2 + k_3)C_E^*(t) \quad \text{(B4)}$$

Multiplying both sides of equation (B4) by $(k_2 + k_3 + k_4)$ gives

$$(k_2 + k_3 + k_4)\frac{dC_i^*}{dt} = K_1(k_2 + k_3 + k_4)C_p^*(t)$$
$$- (k_2 + k_3 + k_4)(k_2 + k_3)C_E^*(t) \quad \text{(B5)}$$

or, equivalently,

$$(k_2 + k_3 + k_4)(k_2 + k_3)C_E^*(t)$$
$$= -(k_2 + k_3 + k_4)\frac{dC_i^*}{dt}$$
$$+ K_1(k_2 + k_3 + k_4)C_p^*(t) \quad \text{(B6)}$$

Taking the derivative of equation (B4) yields

$$\frac{d^2 C_i^*}{dt^2} = K_1\frac{dC_p^*}{dt} - (k_2 + k_3)\frac{dC_E^*}{dt} \quad \text{(B7)}$$

Substituting equation (B1) into (B7), that is,

$$\frac{d^2 C_i^*}{dt^2} = K_1\frac{dC_p^*}{dt} - (k_2 + k_3)$$
$$\times [K_1 C_p^*(t) - (k_2 + k_3 + k_4)C_E^*(t)] \quad \text{(B8)}$$

and equation (B6) into (B8) leaves

$$\frac{d^2 C_i^*}{dt^2} = -(k_2 + k_3 + k_4)\frac{dC_i^*}{dt}$$
$$+ K_1\frac{dC_p^*}{dt} + K_1 k_4 C_p^*(t) \quad \text{(B9)}$$

Twice integrating equation (B9) provides the basis for linear estimation of the parameters:

$$C_i^*(T) = -\theta_1 \int_0^T C_i^*(t)dt$$
$$+ \theta_2 \int_0^T C_p^*(t)dt + \theta_3 \int_0^T \int_0^t C_p^*(s)ds\,dt \quad \text{(B10)}$$

where

$$K_1 = \theta_2,$$
$$k_2 + k_3 = \theta_1 - (\theta_3/\theta_2) \text{ and } k_4 = (\theta_3/\theta_2) \quad \text{(B11)}$$

Although $C_i^*(t)$ is not directly measured by the PET camera, is can be estimated by correcting the total activity measured by the PET camera, $C_T^*(t)$, for the labeled CO_2 in brain and the activity in the blood in the brain, as described in equations (11) and (12), that is,

$$C_i^*(t) = C_E^*(t) + P^*(t)$$
$$\approx \frac{C_T^*(t) - V_b C_b^*(t)}{(1 - V_b)} - V_D C_a^*(t) \quad \text{(B12)}$$

where V_D is the equilibrium distribution ratio for labeled CO_2, V_b is the blood volume, and $C_b^*(t)$ is the total blood activity.

When V_D and V_b are known, the time course of $C_i^*(t)$ can be determined from equation (B12) and a linear least-squares procedure can be used to estimate θ_1 through θ_3, and hence the rate constants for leucine and λ. In the estimation, we assume that either V_D is known or that $V_D C_a^*(t)$ is sufficiently small compared with $C_T^*(t)$ that labeled CO_2 in the tissue can be ignored, that is, fitting can proceed with $V_D = 0$. When V_b is unknown, the fitting procedure can be applied for a range of values of V_b and the best fitting solution chosen. Finally, requiring that K_1 be positive, and that $k_2 + k_3$ and k_4 be non-negative, leads to constraints

$$\theta_2 > 0 \text{ and } \theta_1\theta_2 \geqslant \theta_3 \geqslant 0 \quad \text{(B13)}$$

In practice, one can apply an unconstrained weighted least-squares algorithm to estimate θ_1 through θ_3, check whether the constraints are met, and in the (usually rare) case that the constraints are not met, re-fit with a more computationally intensive constrained minimization algorithm. In the present study, the constrained minimization program from Matlab® (The Mathworks Inc., Natick, MA, USA) was used when parameters estimated by unconstrained linear least squares did not meet the conditions in equation (B13).